Table 2 Estimated state vector at fourth-stage ignition of a satellite launch vehicle

	Altitude, km	Range, km	Relative velocity, km/s	Relative flight path angle, deg	Relative flight azimuth, deg
Coat phase dc (Ref. 4)	304.7	1035.9	3.849	1.394	137.726
Present method	305.6	1035.0	3.846	1.467	137.714

Rapid convergence is obtained in each cycle with an error tolerance of 0.01 units. Parametric studies have been carried out on different sampling rates varying from 10 to 1 Hz and for span variations from 2 to 10 s. The estimated trajectory parameters with 5-s span and a 10-Hz sampling rate are very close to the simulated trajectory. The computed random errors in the measurements show the same magnitude as that used for simulation. In the case of actual tracking data, preprocessing for bias removal, wild samples editing, etc., are necessary prior to actual application.

Application to Sounding Rockets

The gravity turn trajectory of a two-stage sounding rocket is reconstructed using preprocessed data of interferometer systems. Data from 3 to 50 s with a 1-Hz sampling rate are considered for trajectory reconstruction. With a 5-s span, the trajectory is reconstructed up to sustainer burnout (50 s). Approximate initial conditions at 3 s are derived from the first few data samples. The estimated state at 50 s is used for coast-phase trajectory propagation until ground impact. The propagated trajectory matches well with that obtained using coast-phase data alone from 50 to 90 s, as in Ref. 4. The trajectory apogee and impact parameters are presented in Table 1. From the estimated unmodeled acceleration, the unmodeled force components are obtained in body frame coordinates (see Fig. 1).

Application to Satellite Launch Vehicles

The preprocessed data of a four-stage solid propellant launch vehicle, from radar system with a 10-Hz sampling rate from 15 to 290 s, is considered for this study. In this case, steering is controlled by preprogrammed orientation angles. A 5-s span is used for trajectory reconstruction up to 190 s (third-stage burnout). The same method is applied to coast-phase data also, but with a 100-s data span. The estimated unmodeled accelerations are found to be of small magnitude ($\simeq 10^{-4}$ m/s^2).

Based on the estimated burnout conditions at 190 s, the long coast trajectory is propagated by numerical integration, and the state vector at fourth-stage ignition (the end of arc) is obtained. In Table 2, this state vector is compared with the results obtained from the differential correction analysis of the coast-phase tracking data alone, as in Ref. 4. The agreement is found to be good. The differential correction analysis during thrust phase, given herein, is thus confirmed by the subsequent coast-phase observations. The reconstructed trajectory parameters such as altitude, range, velocity, flight-path angle, and azimuth angle are shown in Fig. 2.

Conclusions

A new approach to the problem of obtaining the trajectory and unmodeled forces from tracking data, applicable for the thrusting phase of sounding rockets and launch vehicles, has been presented. The examples show the new method is very versatile. The differential correction algorithm has the advantage of simplicity, modest computational requirements, and fast convergence. The unmodeled acceleration gives an idea of the unaccounted force components as well. The new method has been used to attain the random errors in the measurements, although this is not reported herein. In general, it can be concluded that this technique is useful in obtaining reasonable estimates of trajectory characteristics of sounding rockets and launch vehicles in near-real time with less effort.

References

[1] Pietrass, A.E., "Digital Filtering Techniques for Real Time Trajectory Estimation and Prediction," 2nd Centro Tecnico Aeroespacial-DFVLR Workshop on Sounding Rockets, Sao Jose Campos, Brazil, Oct. 1976.

[2] Bryson, A.E., "Kalman Filter Divergence and Aircraft Motion Estimations" *Journal of Guidance and Control,* Vol. 1, Jan.-Feb. 1978, pp. 71-79.

[3] Chapman, G.T. and Kirk, D.B., "A Method of Extracting Aerodynamic Coefficients from Free Flight Data," *AIAA Journal,* Vol. 8, April 1970, pp. 753-758.

[4] Janardana Rao, Y., Sreehari Rao, Ch., and Pillai, S.K., "Trajectory Estimation from Tracking Data of Sounding Rockets using the Method of Differential Correction," *Proceedings of AIAA 4th Sounding Rocket Technology Conference,* Boston, Mass., June 1976, pp. 1-11.

Optimal Controller for Homing Missile

William R. Yueh*
Northrup Electronics Division
Hawthorne, California
and
Ching-Fang Lin†
Boeing Military Airplane Company
Seattle, Washington

Introduction

OPTIMAL control theory is applied to the homing missile lateral autopilot design. The approach is to adapt the autopilot gains to the environment model reference and to vary as functions of time-to-go to minimize the performance index. The path constraint is applied throughout the whole terminal homing period and infinite penalty is imposed at intercept. A single-plane, linear autopilot design and implementation consideration are addressed for the skid-to-turn (STT) case.

The controller for a homing missile, in general, is a closed-loop system called "autopilot," which is a minor loop inside the main guidance loop. In addition to the control surface and servomechanism, the autopilot consists of mainly the accelerometers and/or (rate) gyros to provide additional feedback into the missile servos to modify the missile motion. Broadly speaking, autopilots either control the motion in the pitch and yaw planes, in which case they are called lateral autopilots, or control the motion around the missile axis and are thus named roll autopilots, and serve quite a different purpose. We address only the lateral autopilot design for the STT case.

The objective here is to outline a single-plane, linear, optimal controller design for varying the autopilot gains to minimize the performance index. With considerations limited to a single plane, we ignore important effects such as roll-yaw

Submitted April 1984; revision submitted June 20, 1984.

*Senior Research Engineer.
†Lead Engineer, Flight Controls Technology. Member AIAA.

coupling and the cross-coupling between pitch and yaw motion. Thus, we have actually assumed that synthetic damping is introduced in both the lateral modes so that the mean pitch and yaw rates are reduced. Also the roll rates are kept low during the lateral maneuvering so that the cross-coupling should be negligible.

It should be noted that in any formulation of an optimal control problem where the Hamiltonian involves the controller in a linear manner only, the application of the Pontryagin's maximum principle will always prescribe a "bang-bang" control. The "bang-bang" or switching control autopilot design requires the input to the rate servo to be a bistable relay which always commands the maximum allowable rates. Because any small signal at the controller input to the relay commands the maximum rate, the equivalent linear gain is extremely high. The high-gain autopilot also has the advantage of being "adaptive" to the environment, since the original airframe characteristics are washed out.

Conceptually, the "bang-bang" controller should render an optimal autopilot design; in practice, however, it suffers multitudinous large problems. The theoretically infinite gain will drive the tail rate signal to zero. It would then dither about zero. The weathercock frequency of the response changes as the square root of the dynamic pressure changes. A high weathercock frequency is essential for the stability of the guidance loop. Thus there will be a stability problem at high altitude. The damping term without being compensated can become unacceptably low for the low altitude case. For large step inputs, the bang-bang controller may require nonlinear compensation to prevent locking into a low-frequency limit cycle oscillation. For a complex system that has additional degrees of freedom such as elastic deformation in the body mode, it requires dither frequency control to prevent structural damage.

In effect, the equivalent high gain has resulted in the roots of the total autopilot system being moved closer to the control zeroes. Thus the autopilot response can revert to that of a linear third-order system.

Linear Third Order System with Trim Aerodynamics

The trim aerodynamics is a steady-state condition of the airframe whereby the moment due to the control surface incidence ν is balanced by the moments due to the angle of attack α.

For each of the combinations that produces zero moments, the airframe flies with constant applied force which is the steady-state (trim) maneuver. By expanding the normal force and moment coefficients in a Taylor series about the trim conditions we can arrive at the following set of simple, linear equations

$$\dot{\gamma}=A\alpha+B\nu \tag{1}$$

$$\ddot{\psi}=C\alpha+D\dot{\psi}+E\nu \tag{2}$$

in terms of the aerodynamic coefficients A to E, which are related to the pertinent stability derivatives. For the pitch autopilot, $\dot{\psi}$ is the missile airframe pitch rate while γ is the velocity angle component in the pitch plane.

The two equations above actually characterize the third order aerodynamics with three perturbed states $(\gamma,\dot{\psi}\ddot{\psi})$ with the angle of attack (α) expressed as

$$\alpha=\psi-\gamma \tag{3}$$

The controller u, as the deterministic input, should be proportional to the control surface incidence angular rate and is expressed as

$$u=E\dot{\nu} \tag{4}$$

The same E coefficient is introduced here to simplify the analytic expressions for the following derivations.

Controller State Parameters

A fourth state is needed to relate the third order autopilot state parameters to the guidance signal. It will be defined as

$$M\equiv -T^2\dot{\sigma}/a \tag{5}$$

where $\dot{\sigma}$ is the geometry line-of-sight (LOS) rate and a is chosen to be $a=A-BC/E\simeq A$ for most cases. T is the time-to-go from intercept.

The LOS angle with radome error induced body motion coupling can be expressed as

$$\sigma=\frac{m}{V_c T}(1+r)-r\psi \tag{6}$$

where m is the lateral miss distance, V_c is the closing speed, and r is the radome error slope parameter. Thus the guidance state M chosen here contains terms proportional to the miss distance and its rate. Hence we can obtain

$$\dot{M}=T\alpha-r_1 T\dot{\psi}+(r_2T^2-b'T)\ddot{\psi} \tag{7}$$

with

$$r_1=\frac{2r+BD/E}{A-BC/E}\simeq\frac{2r}{A} \tag{8}$$

and

$$r_2=\frac{r}{A-BC/E}\simeq\frac{r}{A} \tag{9}$$

and

$$b'\equiv\frac{b}{a}\equiv\frac{B}{aE}=\frac{B}{AE-BC}\sim\frac{B}{AE} \tag{10}$$

To facilitate a closed-form analytic expression for the optimal control, reasonable approximations will be introduced. First, the rate of change of the angle of attack can be approximated to be the body pitch rate, since body flailing always dominates the velocity angle rate. Also, as can be justified by the final results, the flight coefficients C and D have negligible effect on the form of the optimal control law except the radome error body motion coupling, which for a typical few-percent coupling, is a higher-order effect and is partially accounted for in Eq. (7). By introducing a new state variable

$$M'=M+b'(\alpha+\dot{\psi}T)-\frac{r}{A}T^2\dot{\psi} \tag{11}$$

Table 1 Optimal control law coefficients

k	Λ	C_1	C_2	C_3
0	2.57	735	153	18
1	2.8	1200	220	22
2	3.03	1827	299	26
3	3.27	2640	390	30
4	3.51	3663	493	34
5	3.76	4920	608	38
6	4	6435	735	42
7	4.24	8232	874	46
8	4.49	10335	1025	50
9	4.74	12767	1188	54
10	4.98	15555	1363	58

we can arrive at a very simple fourth order controller state equation for the state vector $x = \text{COL}\,[M', \alpha, \dot{\psi}, \ddot{\psi}]$, i.e.,

$$\frac{dx}{dt} = Ax + au \tag{12}$$

with

$$A = \begin{bmatrix} 0 & T & 0 & 0 \\ 0 & 0 & 1 & 0 \\ 0 & 0 & 0 & 1 \\ 0 & 0 & 0 & 0 \end{bmatrix} \tag{13}$$

and

$$a = \text{COL}\,[0,\ 0,\ 0,\ 1] \tag{14}$$

Optimal Control Law

The control law will be derived analytically by minimizing the performance index

$$J = \int_0^{T_H} u^2 \cdot T^{-k} dt \tag{15}$$

where the path constraint is applied throughout the whole terminal homing phase with T_H being the homing time.

The innovation lies in the choice of the penalty function which is inversely proportional to the Kth (integer) power of time-to-go. Using the adjoint techniques in Ref. (1) by first integrating the decoupled co-state equations backward in time, then taking advantage of the regularity in the descending series of powers in T for the 4×4 weighting coefficient matrix, the optimal controller can be derived as

$$u = \frac{1}{T^3}\left[C_1(\alpha - \alpha_c) + C_2 T\dot{\psi} + C_3 T^2 \ddot{\psi}\right] \tag{16}$$

The "commanded" angle of attack α_c introduced here is proportional to the guidance state M' by

$$\alpha_c = -\Lambda \frac{V_c}{V_m}\frac{M'}{T^2} \tag{17}$$

The commanded acceleration $n_c = V_m \dot{\gamma}_c \simeq V_m A \alpha_c$ can be expressed as

$$n_c = \Lambda V_c\left[(\dot{\sigma} + r\dot{\psi}) - \frac{B}{E}\left(\frac{\dot{\psi}}{T} + \frac{\alpha}{T^2}\right)\right] \tag{18}$$

Thus the optimal controller is related to a modified proportional navigation system with navigation ratio Λ. Besides the small trim aerodynamic correction term that is proportional to B/E (<0.01), there is also the pitch rate compensation term which accounts for the radome error.

To alleviate the severe radome stability problem for a high-altitude engagement scenario, one of the commonly used engineering "fixes" is to introduce pitch rate compensation $K_r\dot{\psi}$ with gain K_r feedback to either before or after the guidance filtering network. It can somewhat symmetrize the positive and negative slope stability region at the cost of slowing down the autopilot response. According to the authors' knowledge, Eq. (18) offers the first analytical expression for a theoretical basis to introduce pitch rate compensation according to the optimal control law provided that the radome error slope can be estimated.

Reference 2 discusses an adaptive real-time estimation scheme using a Kalman filter bank design for the switching environment with a built-in "learning" process for in-flight radome error calibration. The radome error slope estimated from the adaptive estimation scheme can be used in Eq. (18) to provide an optimal pitch rate compensation scheme for the optimal controller. To be consistent with the single plane analysis, here only the in-plane slope estimates are needed.

Equations (15) and (16) show that an infinite penalty is assigned at intercept ($T=0$) for k being a positive integer for the three autopilot state parameters, i.e., angle of attack (or the velocity angle rate), pitch rate and pitch acceleration, and the guidance state M'. The latter is proportional to the line-of-sight (LOS) rate besides the other terms discussed previously. Were the truth model identical to the fourth order system, the LOS rate (plus the radome coupling term) would be brought to null and the autopilot states to rest at intercept. The optimal control law thus derived can minimize the RMS miss, terminal angle of attack, pitch rate and the control surface "flapping" rate in the presence of unmodeled errors.

Reduced RMS miss distance can increase the hit probability while reduced angle of attack near intercept can increase the overall kill probability for the favorable endgame study.

The control law coefficients C_i's, $i=1,2,3$ and Λ have been derived analytically for integral values of k and are presented in Table 1.

The $k=0$ case, which corresponds to unity penalty function in Eq. (15), renders a navigation ratio too small to be used. The value compatible with the optimal guidance as a predicted proportional navigation scheme is associated with the $k=6$ case.

Implementation Considerations

For the actual implementation of this optimal controller with a third-order autopilot, Eq. (16) will be cast in the following form:

$$\dot{\nu} = -K_0\tilde{n}_c + K_1 n + K_2\dot{\psi} + K_3\ddot{\psi} \tag{19}$$

where the nominal command acceleration is written as

$$\tilde{n}_c = \Lambda V_c(\dot{\sigma} + \hat{r}\dot{\psi}) \tag{20}$$

with the estimated radome error slope $\hat{r}$ as an input to the controller by using the separation principle. The optimal autopilot gains can be expressed as the following, with $b' \equiv B/AE$,

$$K_1 = \frac{C_1}{V_m A E T^3}\left(1 + \Lambda\frac{V_c}{V_m}b'\frac{1}{T^2}\right) \tag{21}$$

$$K_2 = \frac{1}{ET^2}\left(C_2 + C_1\Lambda\frac{V_c}{V_m}b'\frac{1}{T^2}\right) \tag{22}$$

$$K_3 = \frac{C_3}{ET} \tag{23}$$

while K_0 is imposed to be

$$K_0 = K_1 + K_2 \tag{24}$$

so that the autopilot always has unity static gain. To avoid any singularity at intercept, a floor is always assumed for time-to-go T. Due to body mode consideration, the gain K_3 should be scaled properly to increase the gain tolerances. For the proportional navigation ratio Λ chosen to be 4, we have $C_1 = 6435$, $C_2 = 735$, and $C_3 = 42$. The flight coefficients A, E, b', and time-to-go T estimates are also required. That is, autopilot gains are functions of time-to-go. The time-to-go information can usually be obtained from the uplink information for command guidance, onboard range information (with Doppler available) or simply countdown from the start of terminal homing. The aerodynamic coefficients are estimated from the conventional adaptive autopilot design, using either the model reference scheme or the parameter identification scheme. From preliminary simulation studies the accuracy required is given by the

following coefficient tolerances: A, 70-120%; E, 50-500%; b', 100-500%; T, 70-120%.

Note that there is great latitude in estimating the flight coefficients E and b'. This flexibility can be used to design a slower autopilot by biasing the estimates upwards. It is recommended from simulation that, during the last quarter second, the commands n_c should be set to zero, which allows the angle of attack to diminish before intercept in order to present a more favorable missile attitude for warhead performance. Actually, the missile attitude at intercept can be set to optimize warhead effectiveness.

Conclusions

Optimal control theory is applied to the linear autopilot pitch plane design of a skid-to-turn missile with consideration for implementation. A closed-form analytic expression of the optimal control law is derived. The autopilot gains are adapted to the environment model reference and varied as functions of time-to-go to minimize the performance index. The path constraint is applied thoughout the whole terminal homing period and infinite penalty is imposed at intercept. The following can result from application of the optimal control law: improvement in miss distance and pitch acceleration history, good immunity to guidance noise, tolerance for radome error, compatibility with short handover times, bringing of autopilot states to rest at intercept, and reduction of the angle of attack at intercept.

Acknowledgment

The authors express special thanks to Dr. F. Reifler of RCA for highlighting some of the preliminary results.

References

[1] Bryson, A.E. and Ho, Y.C., *Applied Optimal Control,* Blaisdell Publishing Co., Waltham, Massachusetts, 1969.

[2] Yueh, W.R., "Adaptive Estimation Scheme for Radome Error Calibration," *Proceedings of the 22nd IEEE Conference on Decision and Control,* San Antonio, Texas, Dec. 1983, pp. 546-551.

Reliability Considerations in the Placement of Control System Components

Raymond C. Montgomery*
NASA Langley Research Center, Hampton, Virginia
and
Wallace E. Vander Velde†
Massachusetts Institute of Technology
Cambridge, Massachusetts

Introduction

FUTURE space missions may involve very large and highly flexible spacecraft. Reference 1 considers a microwave radiometer 100 m in diameter. In that example, many actuators and sensors were needed to meet radiometry requirements. Also, to amortize the mission costs, mission life is ideally 20 years or more with occasional revisits for repair and replacement. One mission, the manned space station, is projected to operate indefinitely. These long-life requirements, large numbers of sensors and actuators, and heavy dependence on the proper operation of the control system call for the design ground rule that components may fail during the mission. Hence, components must be placed effectively on the structure and on-line automatic failure detection, identification, and control system reconfiguration (FDI&R) capability is needed. Unfortunately, this capability at the overall system level is still in the research stage. Until now, advanced redundancy management techniques have been used only in research programs. For example, the NASA F8-DFBW program demonstrated analytic redundancy management of sensors in a high-performance research aircraft.[2] In that activity, the problem was simpler than the current one since flexibility was not an overbearing issue.

The problem of selecting component locations is addressed in this paper. The goal is to provide the designer a method of evaluating different sets of locations with regard to their performance as it affects component reliability. This was done in Ref. 3 for the problem of static shape control of a beam. In that paper, optimal locations of force actuators on a beam were found to bend the beam to fit a prescribed parabolic shape. It was shown that reliability should have substantial impact on the selection of the locations of the actuators. This concept has been applied to static shape control of a grid in Ref. 4. Therein the criterion was shown to favor clustering the force actuators for long-life missions, since any one may substitute for the others. For short-life missions (or missions where reservicing can be conducted frequently), physically distributing the actuators is favored.

This Note extends the approach of Ref. 4 to dynamic vibration suppression and applies the theory developed to a grid. Reference 5 treats the problem by constructing a measure of controllability and suggests optimizing the average value of that measure taken over the design mission life. Herein, vibration suppression is treated using optimal regulator theory. First, the general discrete regulator theory is overviewed. Then, the reliability of the components is considered and the failure characteristics of the components are modeled. Finally, results of the analysis are presented that compare the performance of actuator location sets on a grid. Optimality is shown to depend on the mission life or reservicing duration interval.

Basic Analytic Considerations

Engineering practice in the modeling of large space structure dynamics has centered around the use of finite element modeling. Herein, such a model is assumed given and valid for the purpose of control system design—the main interest here

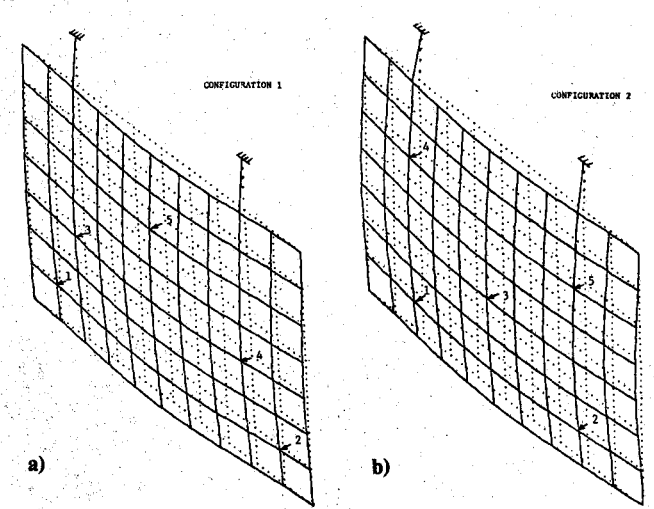

Fig. 1 Two sets of actuator locations considered: a) configuration 1; b) configuration 2.

Presented as Paper 83-2260 at the AIAA Guidance and Control Conference, Gatlinburg, Tenn., Aug 15-17, 1983; submitted April 13, 1984; revision submitted Aug. 15, 1984. This paper is declared a work of the U.S. Government and therefore is in the public domain.

*Aerospace Technologist, Spacecraft Control Branch. Member AIAA.

†Professor of Aeronautics and Astronautics, Department of Aeronautics and Astronautics. Fellow AIAA.